

Supporting Information

Mechanistic insights into high-throughput screening of tandem catalysts for CO₂ reduction to multi-carbon products

Yingnan Liu,^a Dashuai Wang,^{*ab} Bin Yang,^a Zhongjian Li,^a Tao Zhang,^f Raul D.
Rodriguez,^e Lecheng Lei^{ab} and Yang Hou^{*abcd}

^a Key Laboratory of Biomass Chemical Engineering of Ministry of Education,
College of Chemical and Biological Engineering, Zhejiang University, Hangzhou
310027, China

^b Institute of Zhejiang University - Quzhou, Quzhou 324000, China

^c School of Biological and Chemical Engineering, NingboTech University, Ningbo
315100, China

^d Hydrogen Energy Institute, Zhejiang University, Hangzhou 310027, China

^e Tomsk Polytechnic University, 30 Lenin Ave, Tomsk 634050, Russia

^f Ningbo Institute of Materials Technology & Engineering, University of Chinese
Academy of Sciences, Ningbo 315200, China

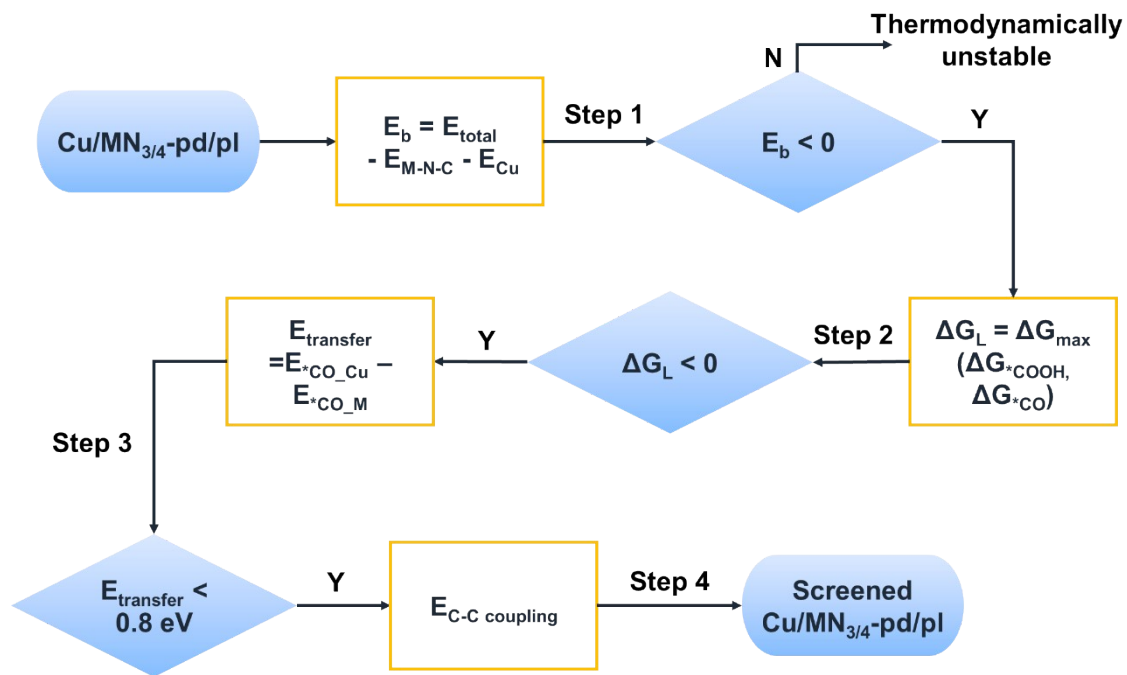


Fig. S1 Schematic diagram of the screening process for selecting optimal tandem catalysts

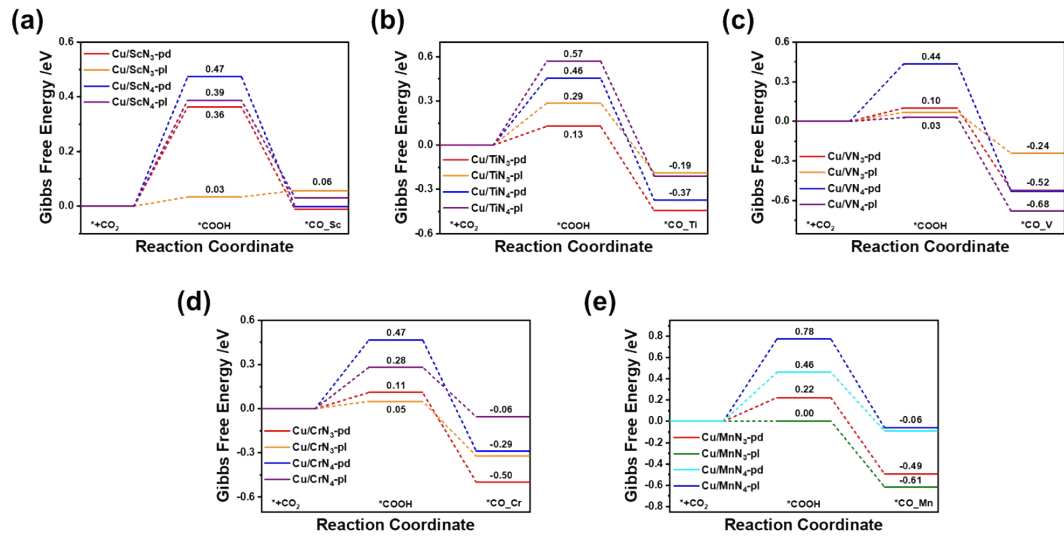


Fig. S2 Gibbs free energy step diagram of reducing CO₂ to *CO on (a) Cu/ScN_{3/4}-pd/pl, (b) Cu/TiN_{3/4}-pd/pl, (c) Cu/VN_{3/4}-pd/pl, (d) Cu/CrN_{3/4}-pd/pl, (e) Cu/MnN_{3/4}-pd/pl.

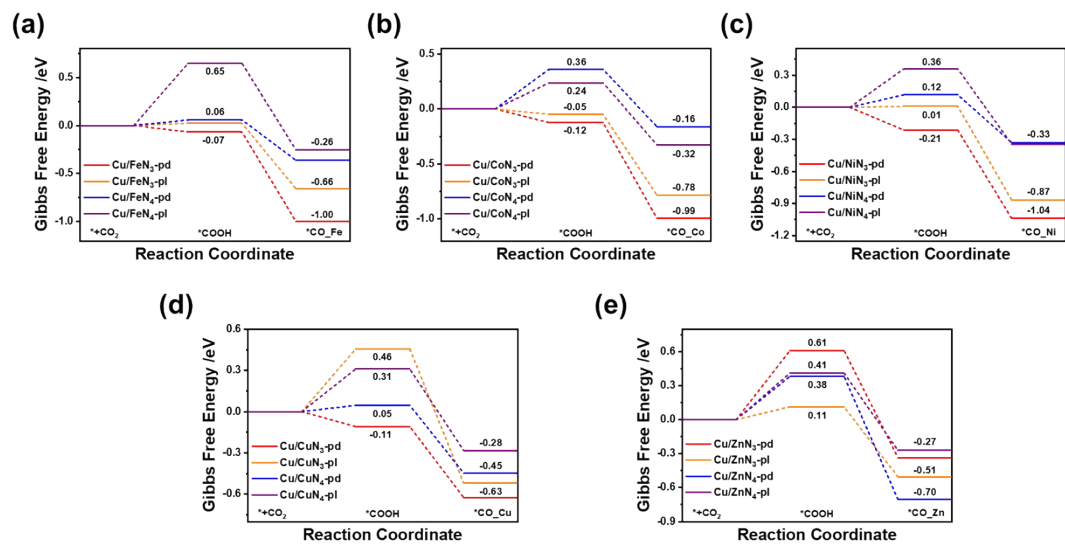


Fig. S3 Gibbs free energy step diagram of reducing CO_2 to $^*\text{CO}$ on (a) Cu/FeN_{3/4}-pd/pl, (b) Cu/CoN_{3/4}-pd/pl, (c) Cu/NiN_{3/4}-pd/pl, (d) Cu/CuN_{3/4}-pd/pl, (e) Cu/ZnN_{3/4}-pd/pl.

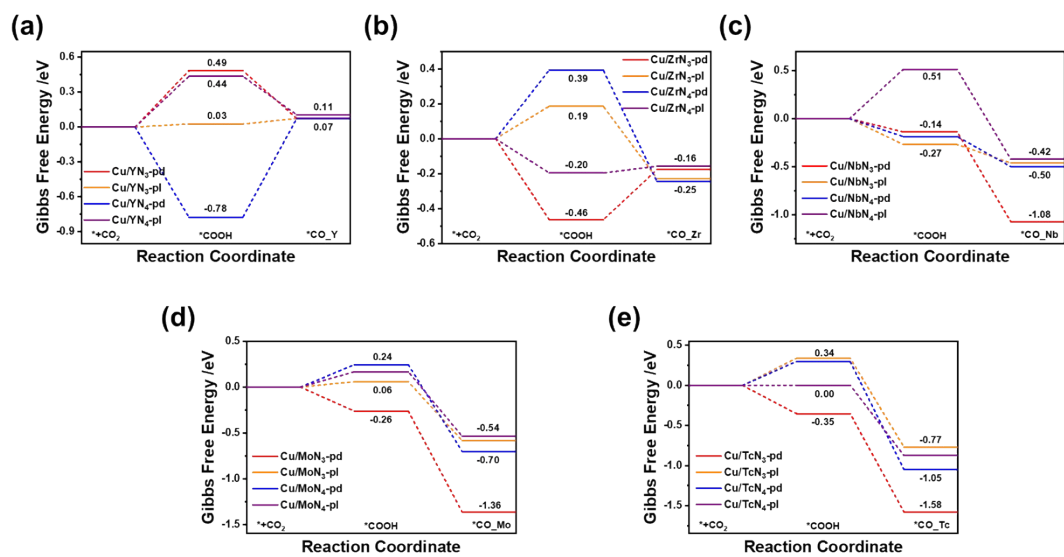


Fig. S4 Gibbs free energy step diagram of reducing CO_2 to $^*\text{CO}$ on (a) Cu/YN_{3/4}-pd/pl, (b) Cu/ZrN_{3/4}-pd/pl, (c) Cu/NbN_{3/4}-pd/pl, (d) Cu/MoN_{3/4}-pd/pl, (e) Cu/TcN_{3/4}-pd/pl.

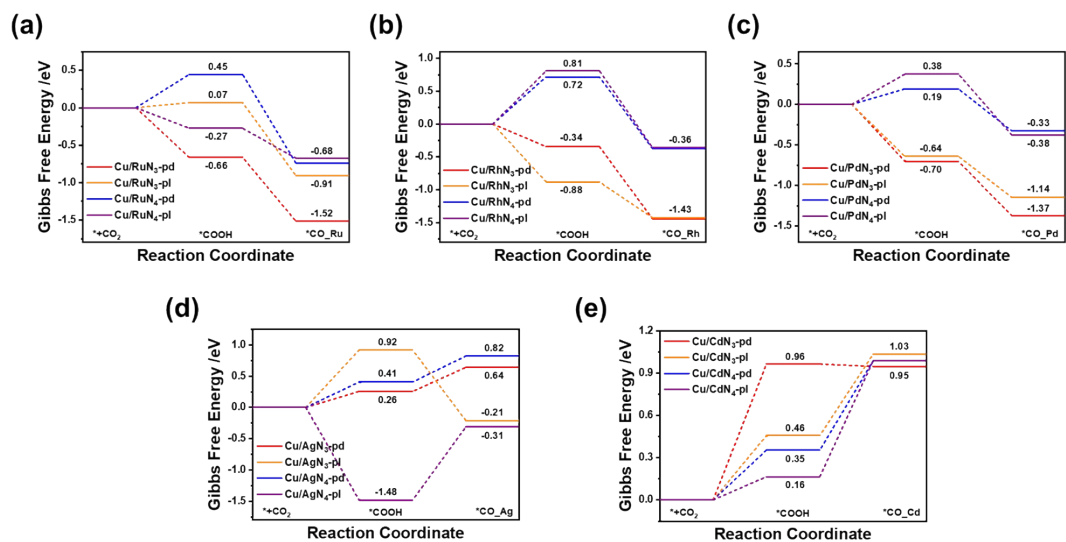


Fig. S5 Gibbs free energy step diagram of reducing CO_2 to $^*\text{CO}$ on (a) Cu/RuN_{3/4}-pd/pl, (b) Cu/RhN_{3/4}-pd/pl, (c) Cu/PdN_{3/4}-pd/pl, (d) Cu/AgN_{3/4}-pd/pl, (e) Cu/CdN_{3/4}-pd/pl.

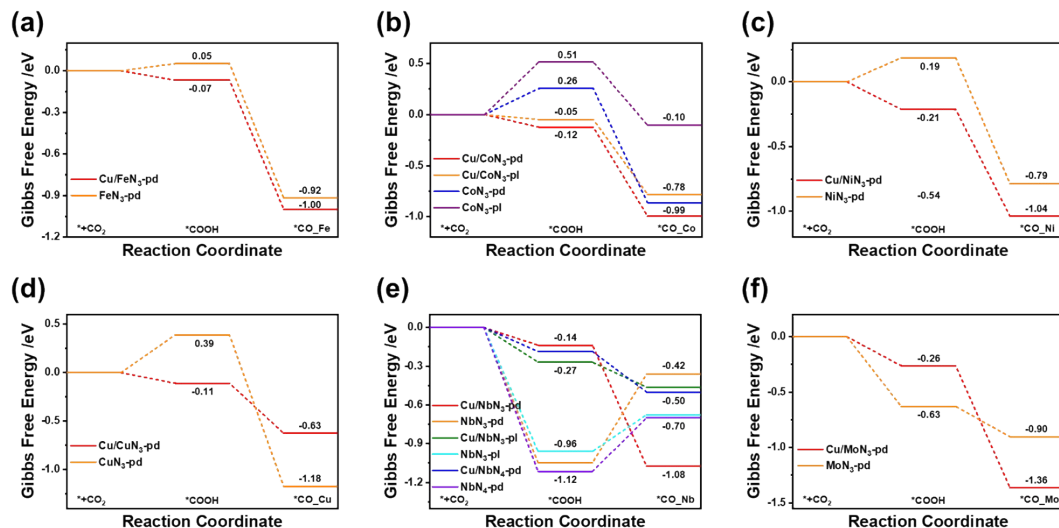


Fig. S6 Gibbs free energy step diagram of reducing CO_2 to $^*\text{CO}$ on (a) Cu/FeN₃-pd and FeN₃-pd, (b) Cu/CoN₃-pd/pl and CoN₃-pd/pl, (c) Cu/NiN₃-pd and NiN₃-pd, (d) Cu/CuN₃-pd and CuN₃-pd, (e) Cu/NbN₃-pd/pl, Cu/NbN₄-pd, NbN₃-pd/pl and NbN₄-pd, (f) Cu/MoN₃-pd and MoN₃-pd.

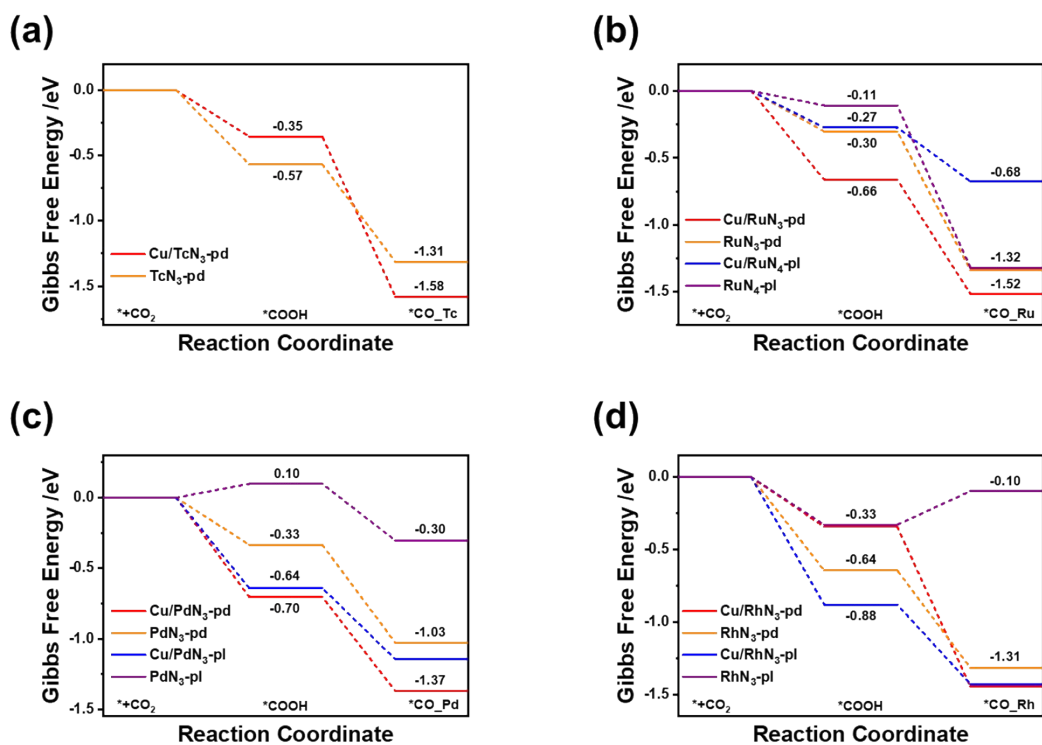


Fig. S7 Gibbs free energy step diagram of reducing CO₂ to *CO on (a) Cu/TcN₃-pd and TcN₃-pd, (b) Cu/RuN₃-pd, Cu/RuN₄-pl, RuN₃-pd and RuN₃-pl, (c) Cu/PdN₃-pd/pl and PdN₃-pd/pl, (d) Cu/RhN₃-pd/pl and RhN₃-pd/pl.

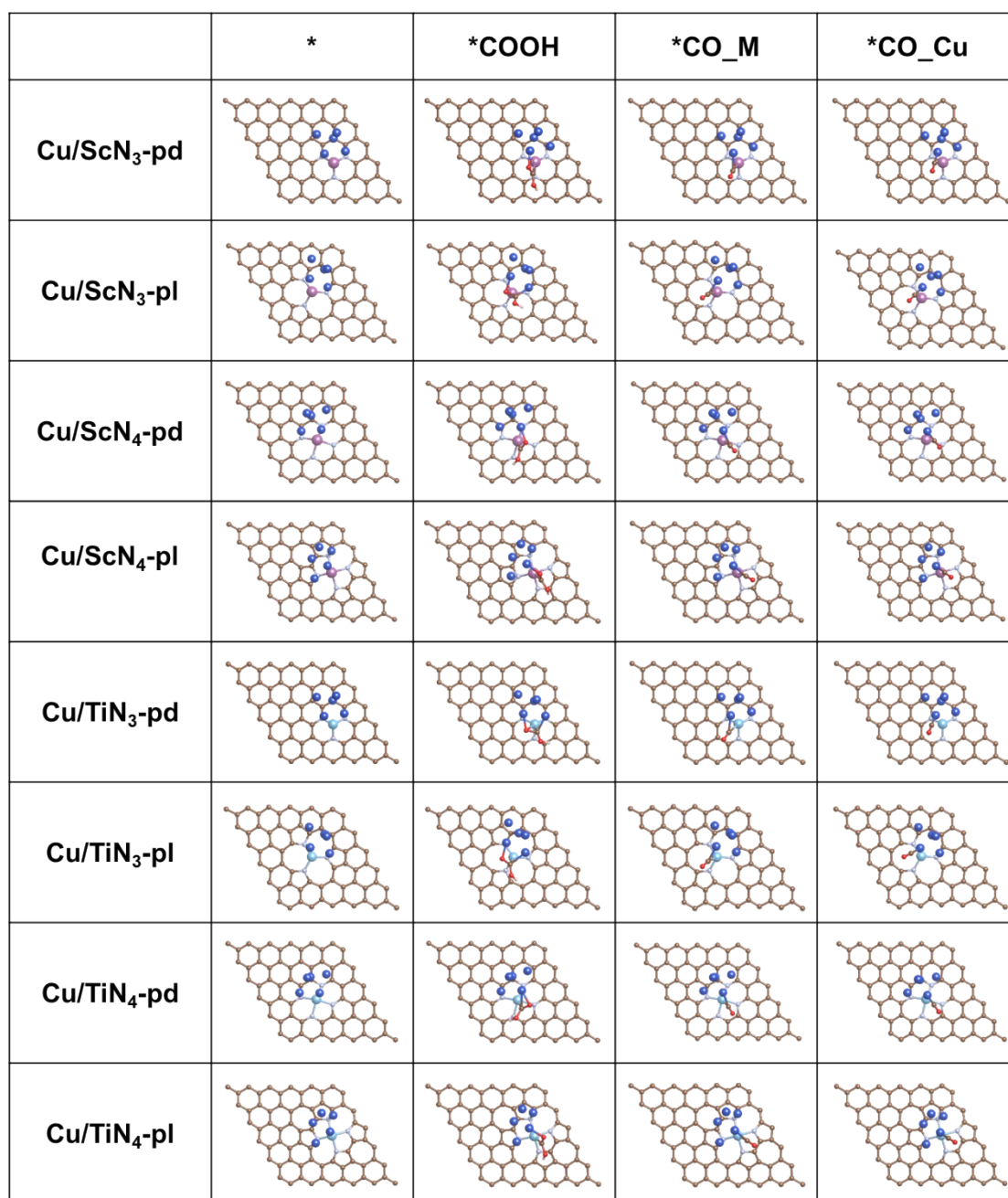


Fig. S8 Model diagrams of different reaction intermediates on the Cu/ScN_{3/4}-pd/pl and Cu/TiN_{3/4}-pd/pl structures.

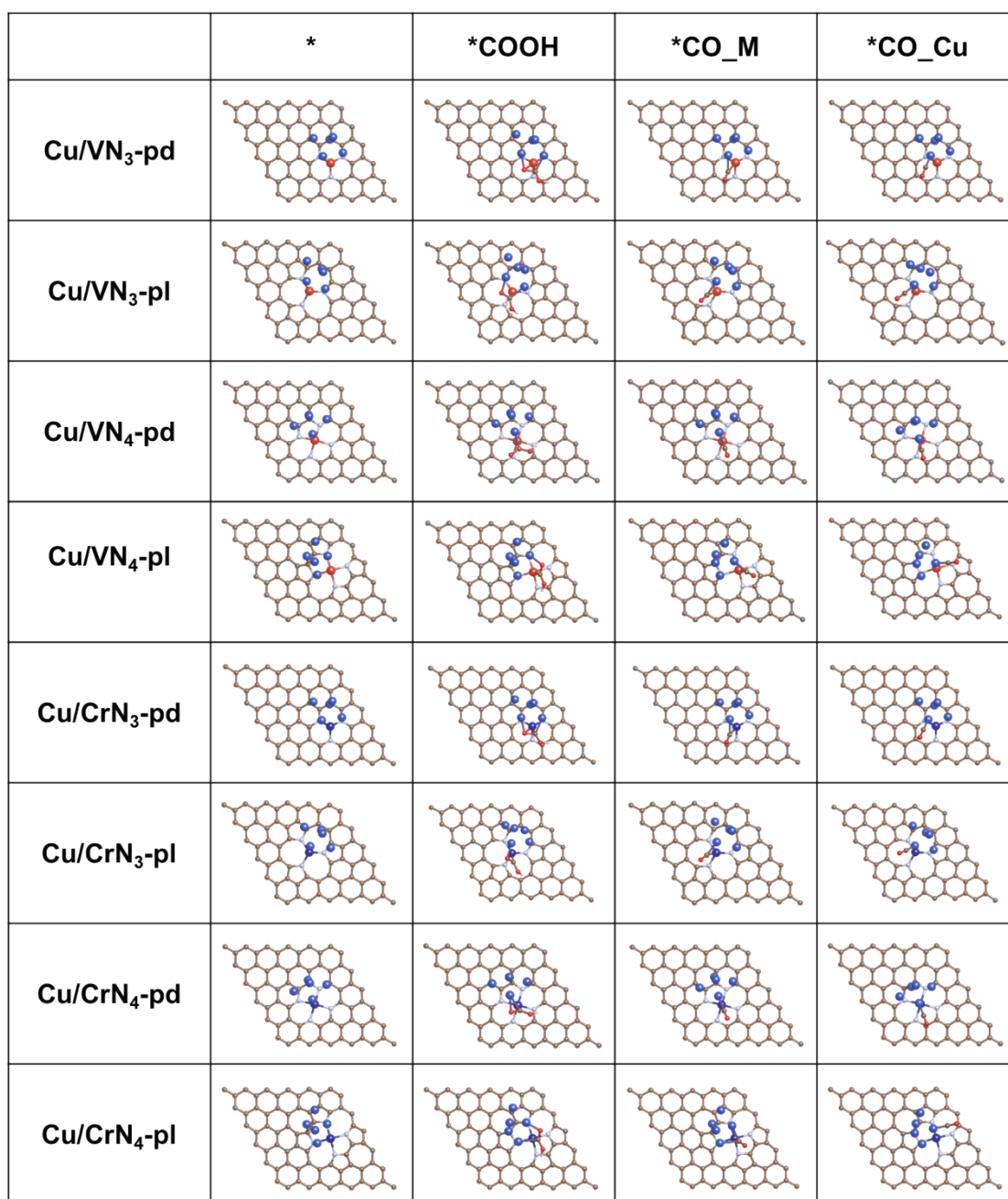


Fig. S9 Model diagrams of different reaction intermediates on the Cu/VN_{3/4}-pd/pl and Cu/CrN_{3/4}-pd/pl structures.

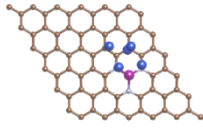
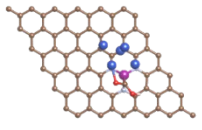
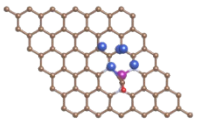
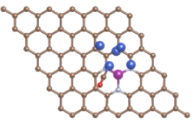
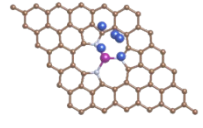
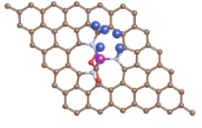
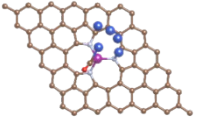
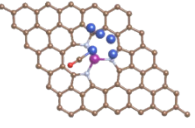
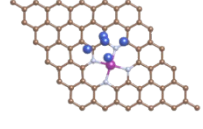
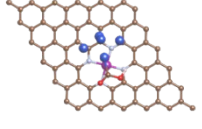
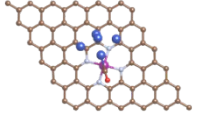
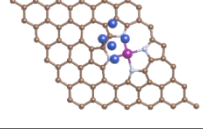
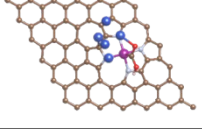
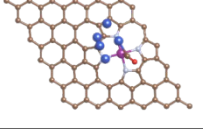
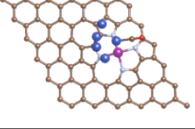
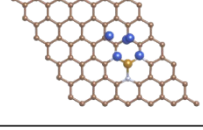
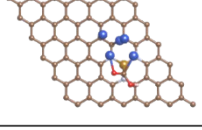
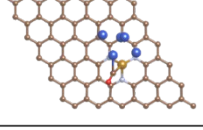
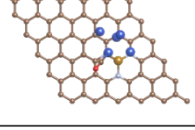
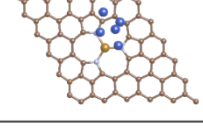
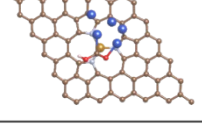
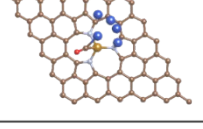
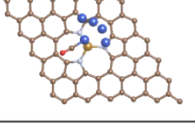
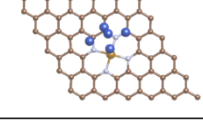
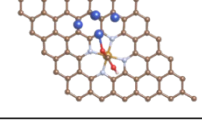
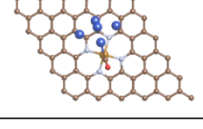
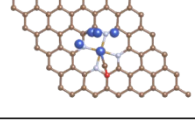
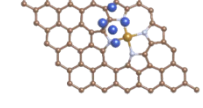
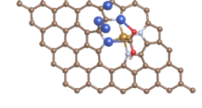
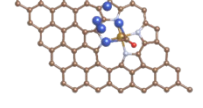
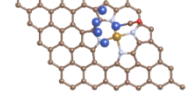
	*	*COOH	*CO_M	*CO_Cu
Cu/MnN₃-pd				
Cu/MnN₃-pl				
Cu/MnN₄-pd				×
Cu/MnN₄-pl				
Cu/FeN₃-pd				
Cu/FeN₃-pl				
Cu/FeN₄-pd				
Cu/FeN₄-pl				

Fig. S10 Model diagrams of different reaction intermediates on the Cu/MnN_{3/4}-pd/pl and Cu/FeN_{3/4}-pd/pl structures.

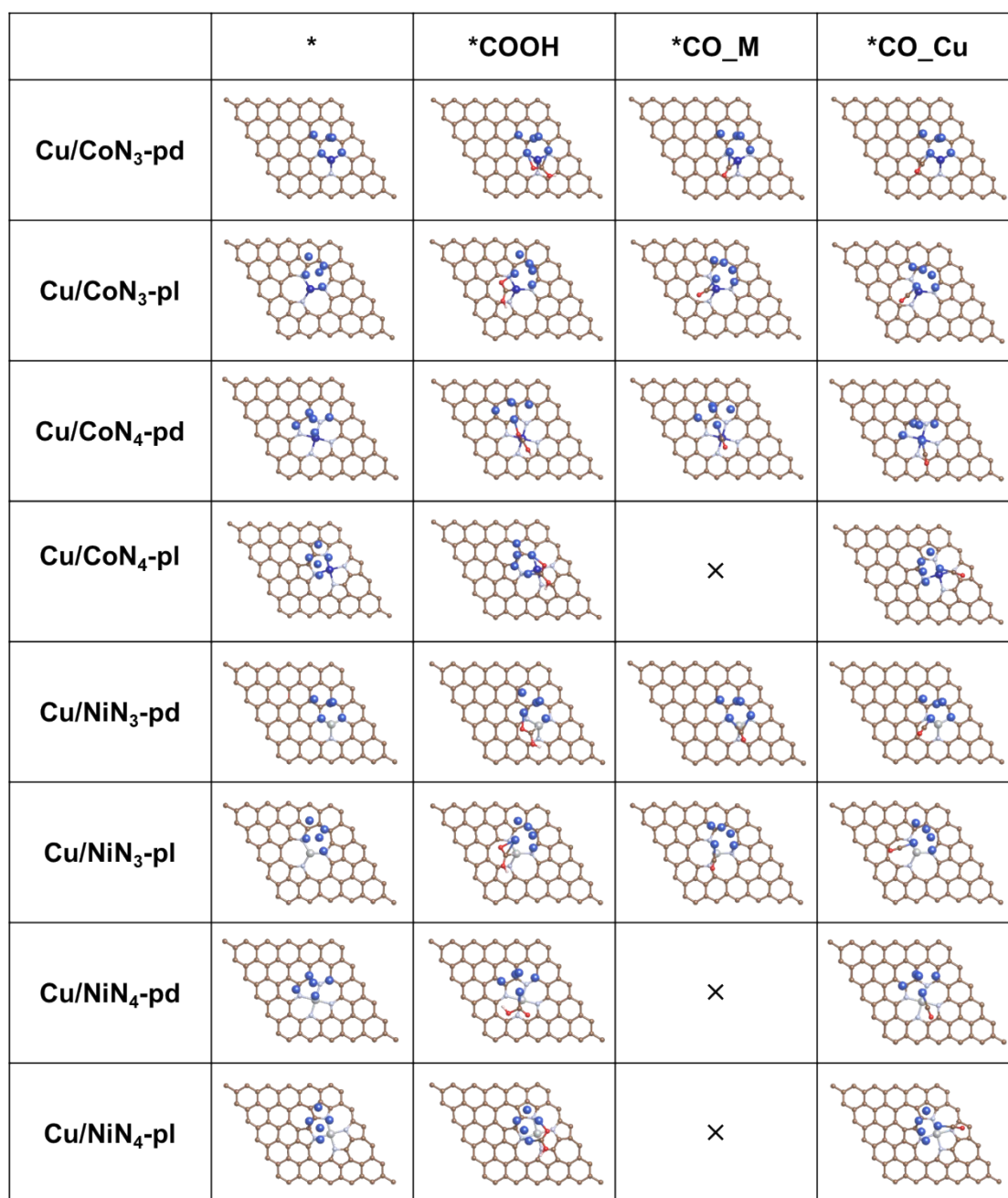


Fig. S11 Model diagrams of different reaction intermediates on the Cu/CoN_{3/4}-pd/pl and Cu/NiN_{3/4}-pd/pl structures.

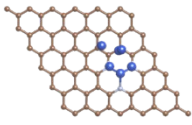
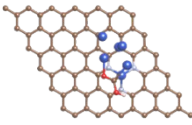
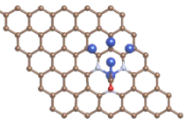
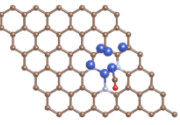
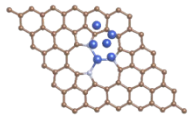
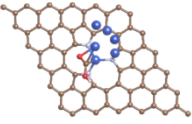
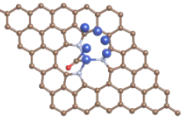
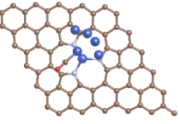
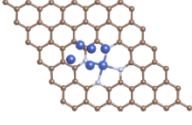
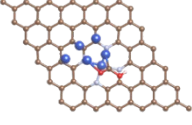
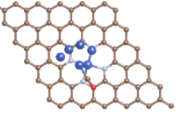
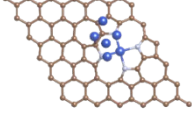
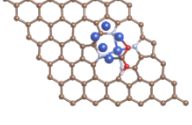
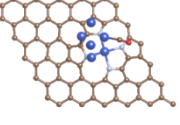
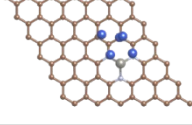
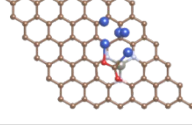
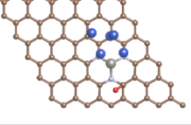
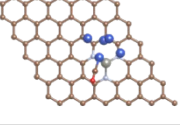
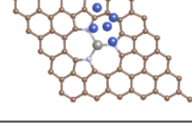
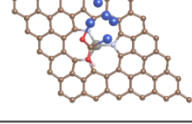
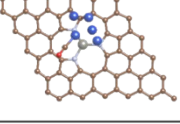
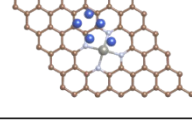
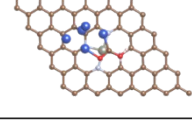
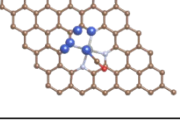
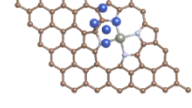
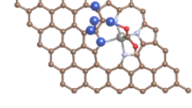
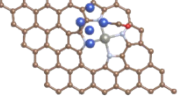
	*	*COOH	*CO_M	*CO_Cu
Cu/CuN₃-pd				
Cu/CuN₃-pl				
Cu/CuN₄-pd			×	
Cu/CuN₄-pl			×	
Cu/ZnN₃-pd				
CuZnN₃-pl			×	
Cu/ZnN₄-pd			×	
Cu/ZnN₄-pl			×	

Fig. S12 Model diagrams of different reaction intermediates on the Cu/CuN_{3/4}-pd/pl and Cu/ZnN_{3/4}-pd/pl structures.

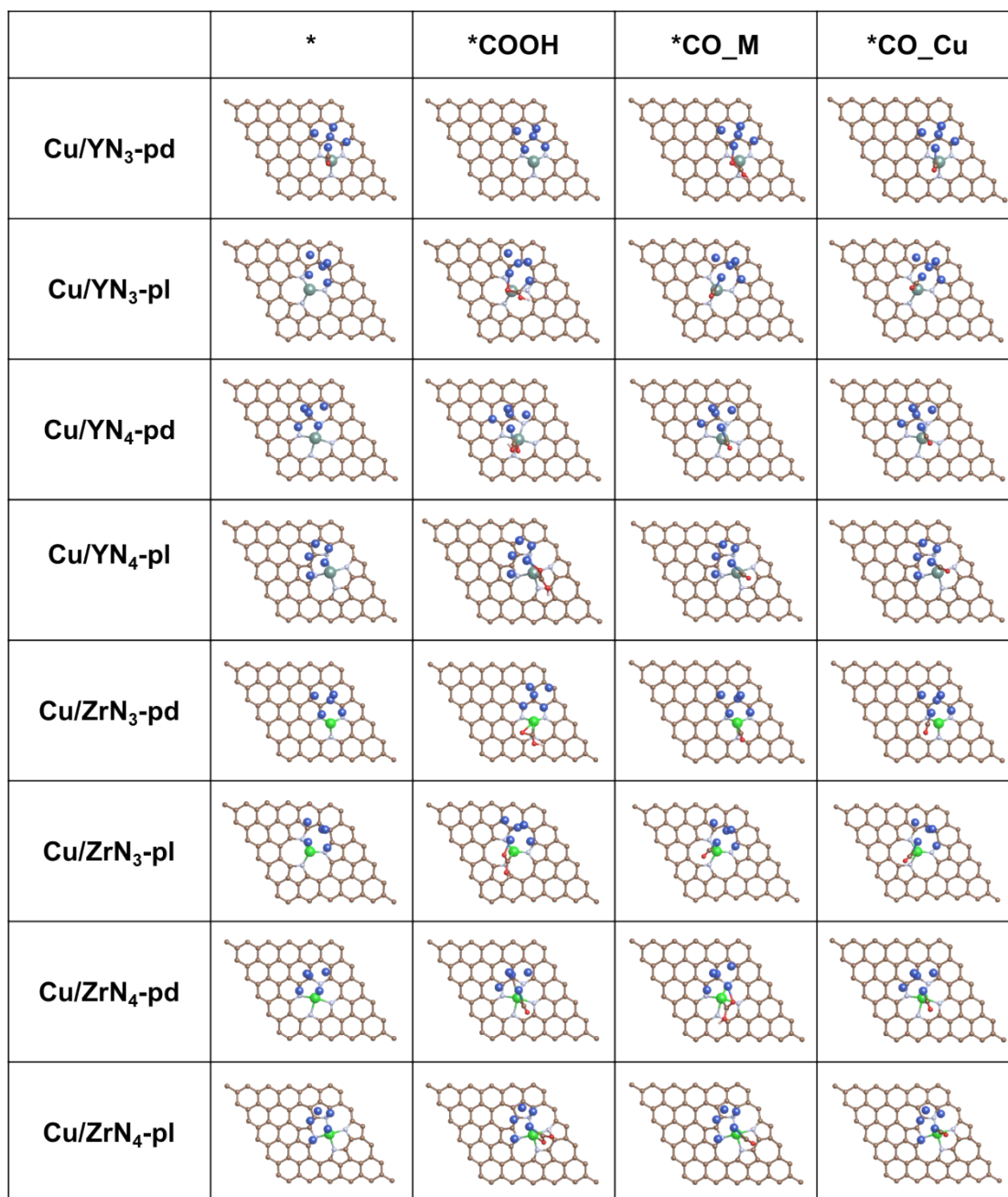


Fig. S13 Model diagrams of different reaction intermediates on the Cu/YN_{3/4}-pd/pl and Cu/ZrN_{3/4}-pd/pl structures.

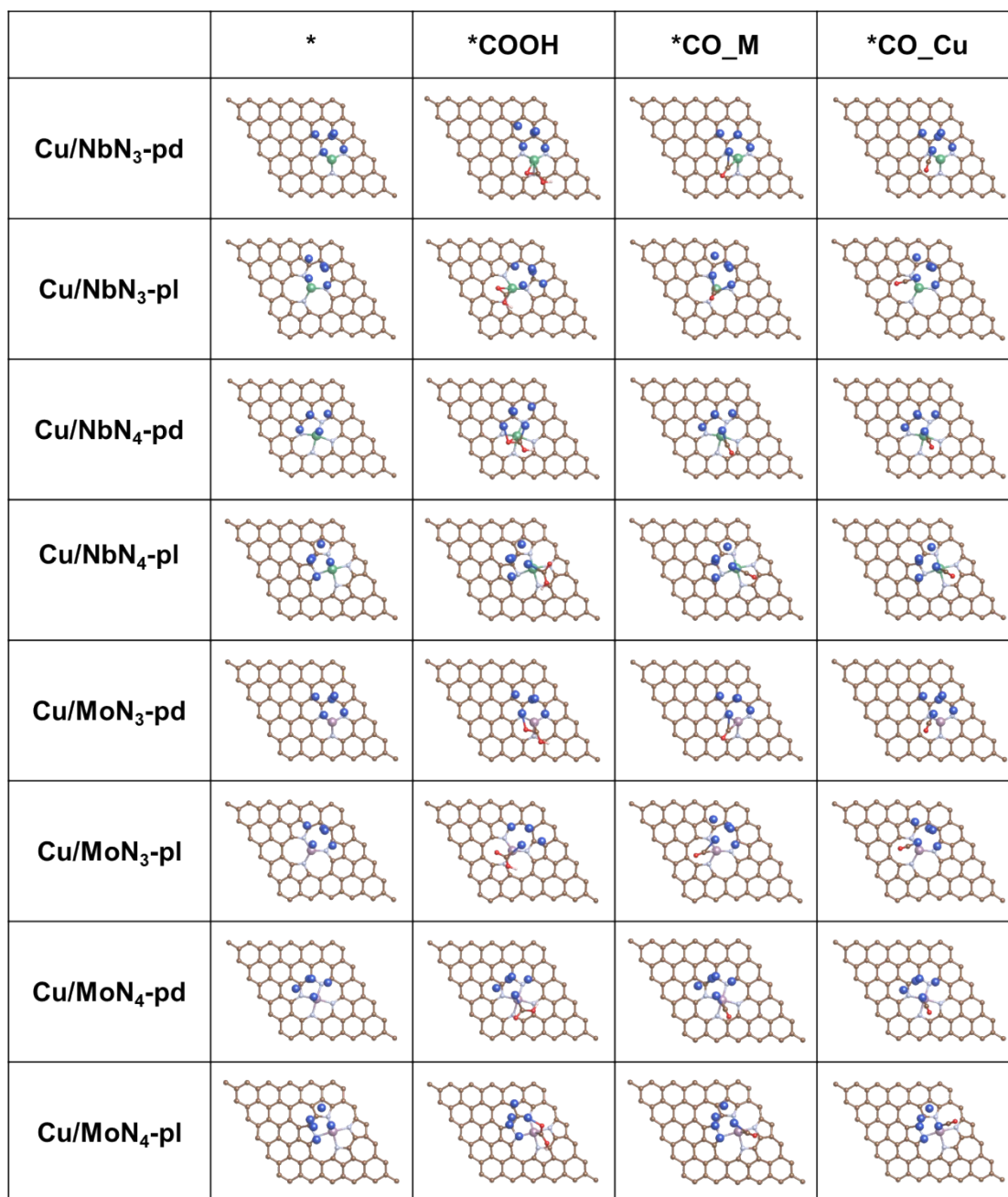


Fig. S14 Model diagrams of different reaction intermediates on the Cu/NbN_{3/4}-pd/pl and Cu/MoN_{3/4}-pd/pl structures.

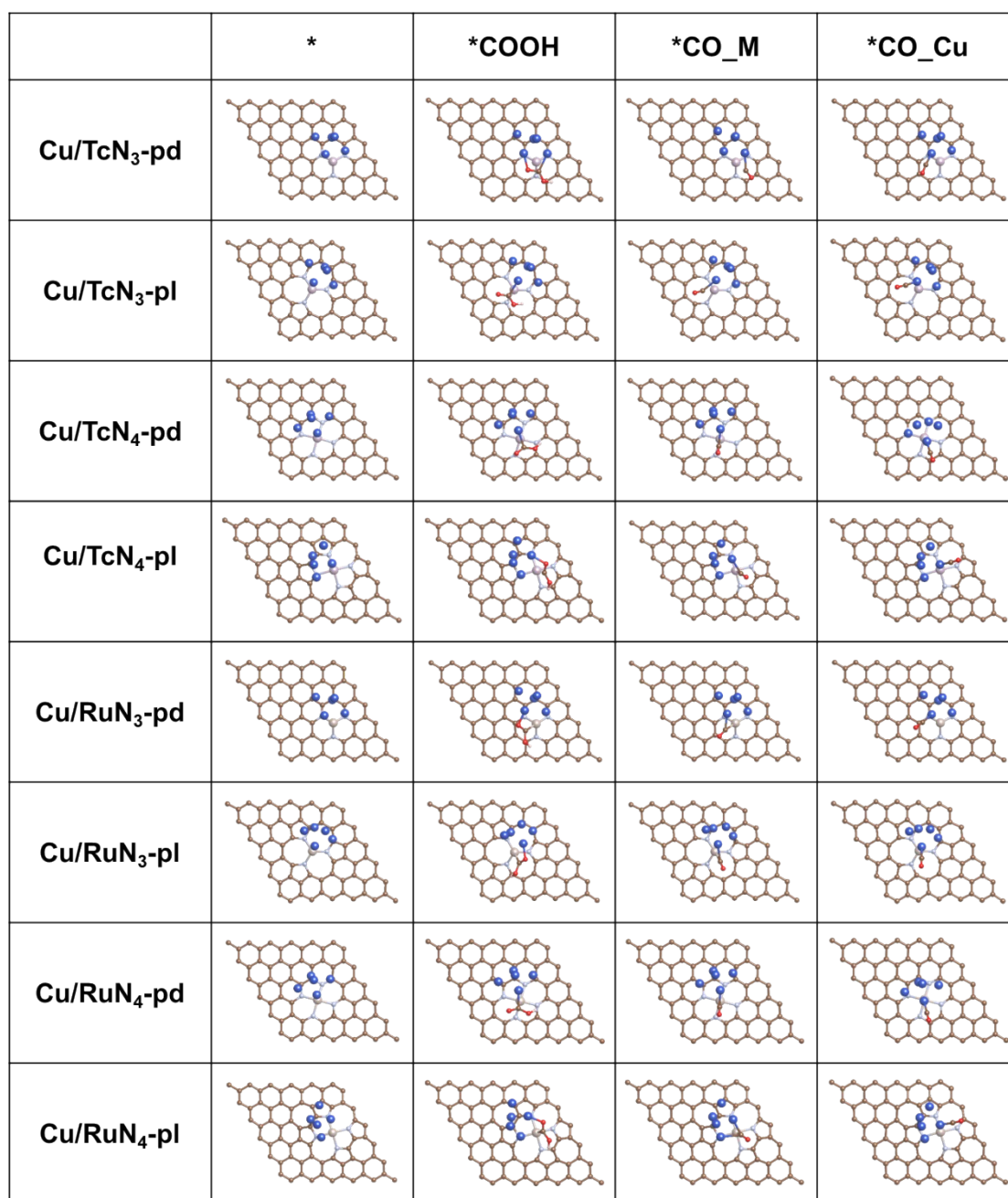


Fig. S15 Model diagrams of different reaction intermediates on the Cu/TcN_{3/4}-pd/pl and Cu/RuN_{3/4}-pd/pl structures.

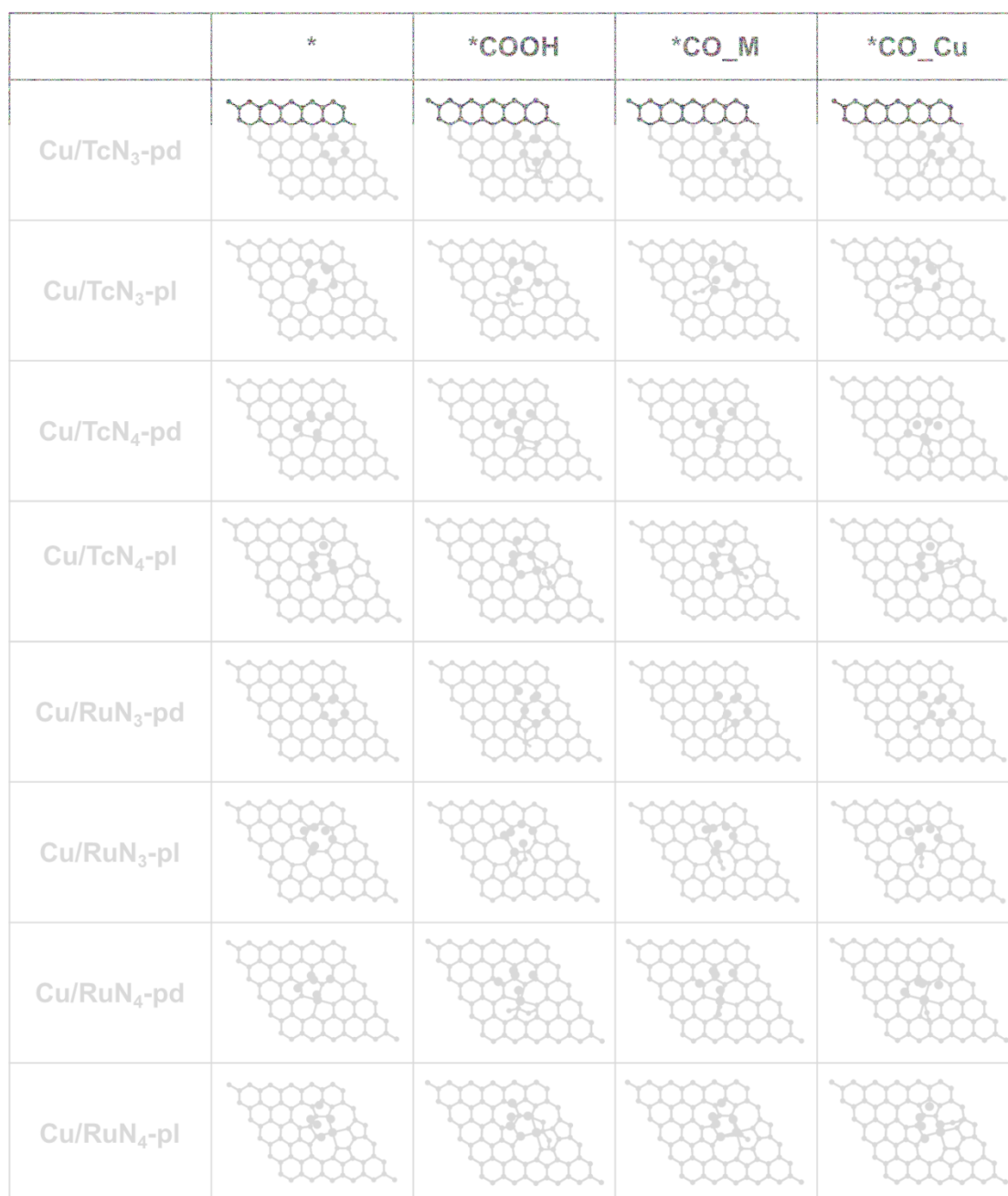


Fig. S16 Model diagrams of different reaction intermediates on the Cu/RhN_{3/4}-pd/pl and Cu/PdN_{3/4}-pd/pl structures.

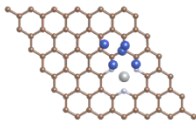
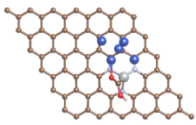
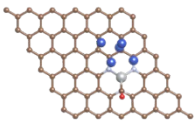
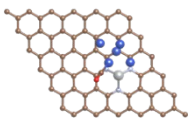
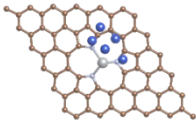
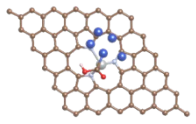
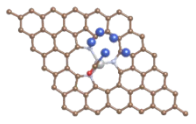
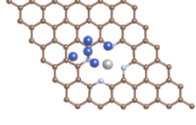
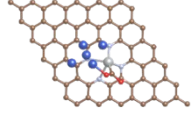
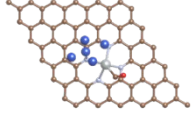
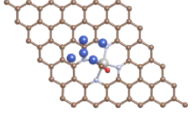
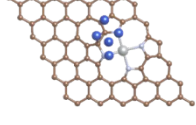
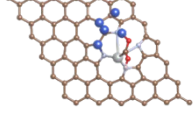
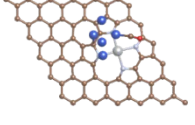
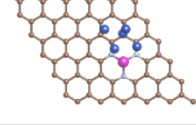
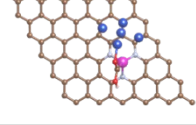
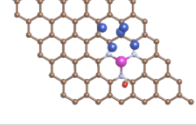
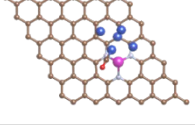
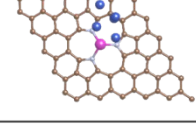
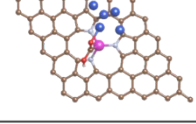
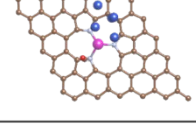
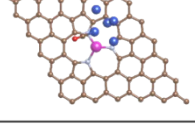
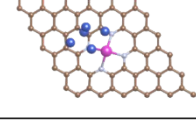
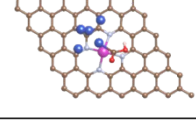
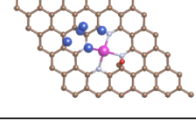
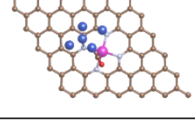
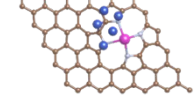
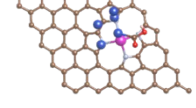
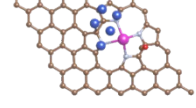
	*	*COOH	*CO_M	*CO_Cu
Cu/AgN₃-pd				
Cu/AgN₃-pl				×
Cu/AgN₄-pd				
Cu/AgN₄-pl			×	
Cu/CdN₃-pd				
Cu/CdN₃-pl				
Cu/CdN₄-pd				
Cu/CdN₄-pl				×

Fig. S17 Model diagrams of different reaction intermediates on the Cu/AgN_{3/4}-pd/pl and Cu/CdN_{3/4}-pd/pl structures.

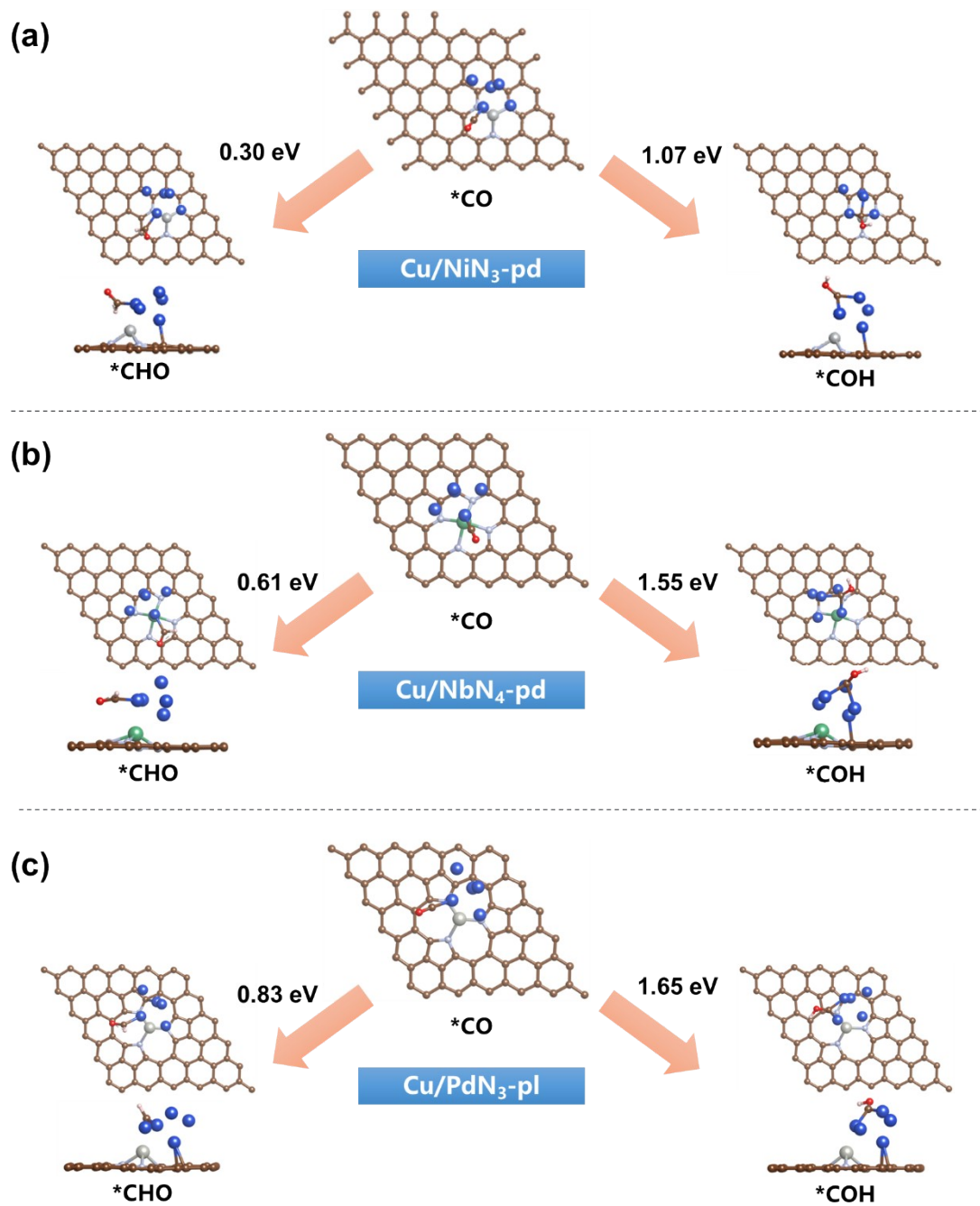


Fig. S18 Schematic diagrams and Gibbs free energy change of *CO hydrogenation conversion to *CHO or *COH on (a) Cu/NiN₃-pd, (b) Cu/NbN₄-pd and (c) Cu/PdN₃-pl, respectively.

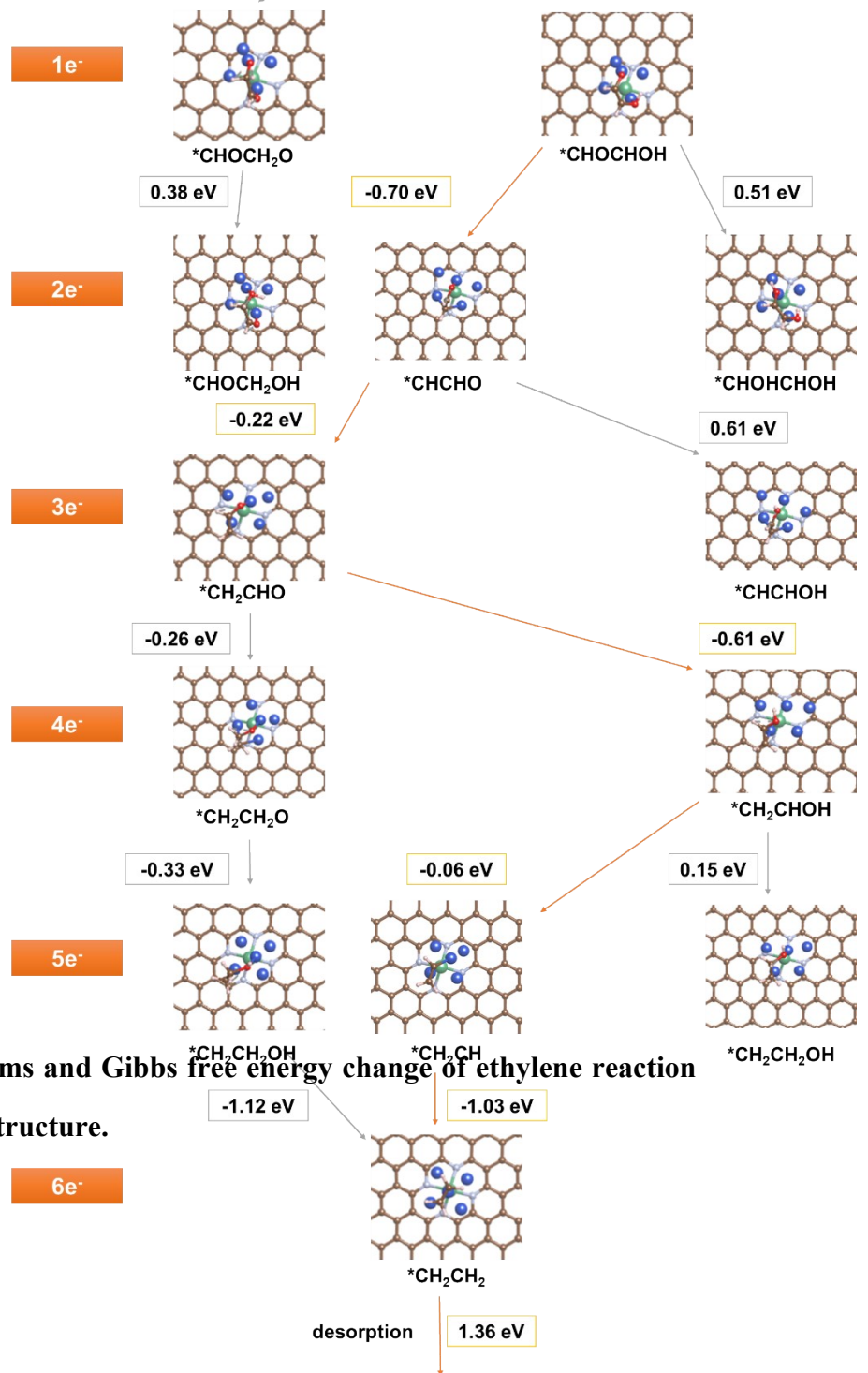


Fig. S19 Schematic diagrams and Gibbs free energy change of ethylene reaction pathway on Cu/NbN₄-pd structure.

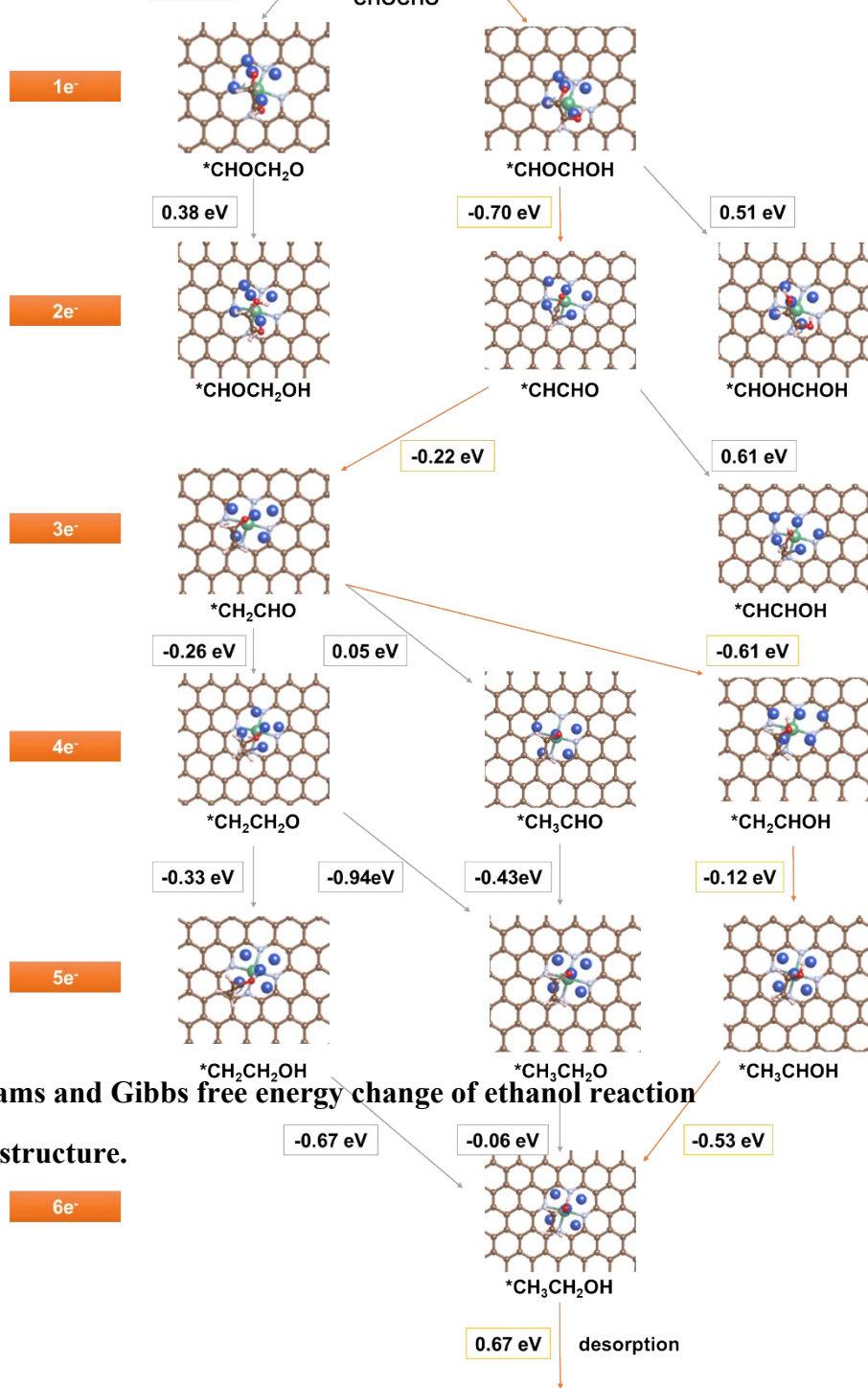


Fig. S20 Schematic diagrams and Gibbs free energy change of ethanol reaction pathway on Cu/NbN₄-pd structure.

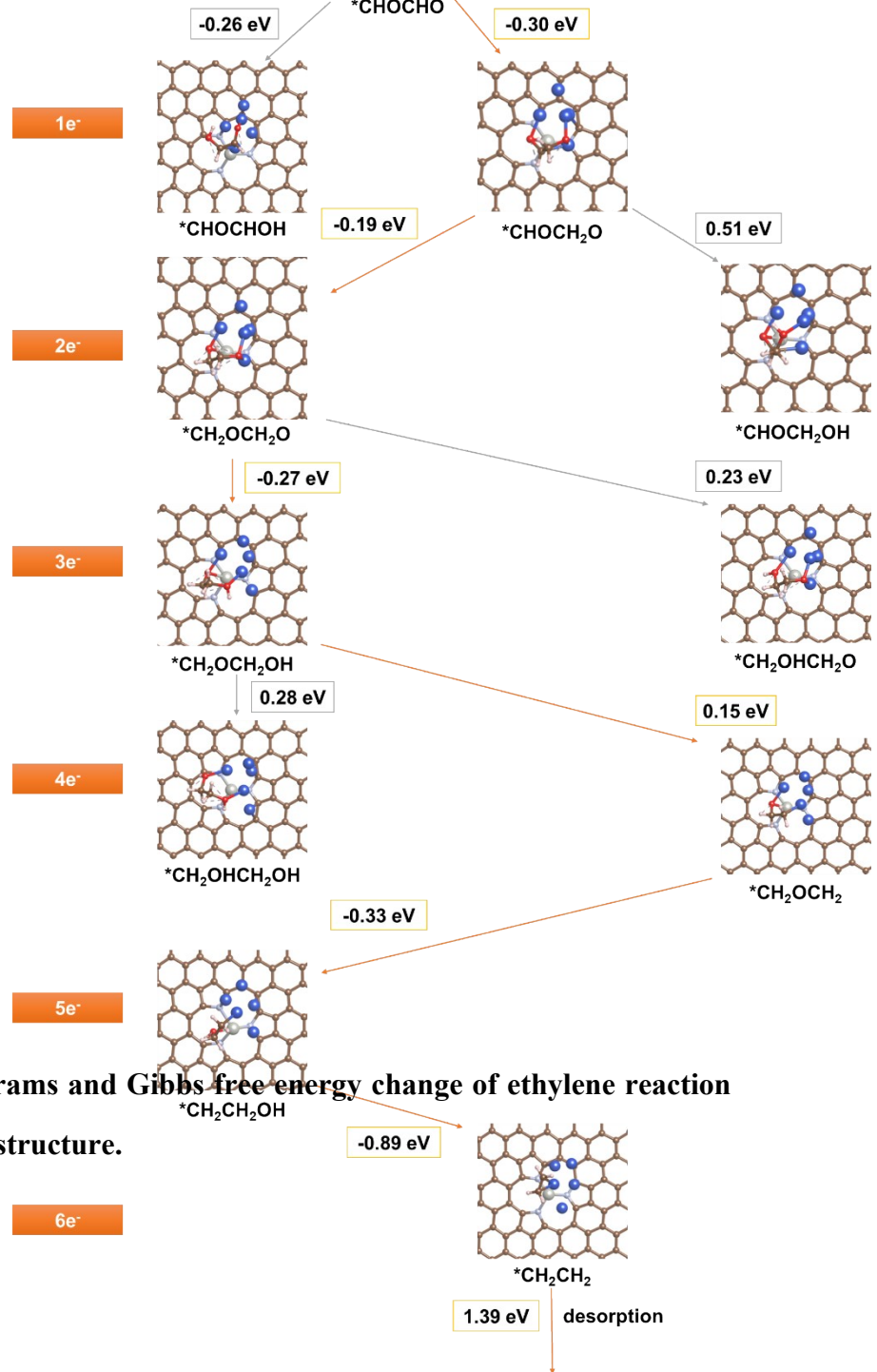


Fig. S21 Schematic diagrams and Gibbs free energy change of ethylene reaction pathway on Cu/PdN₃-pl structure.

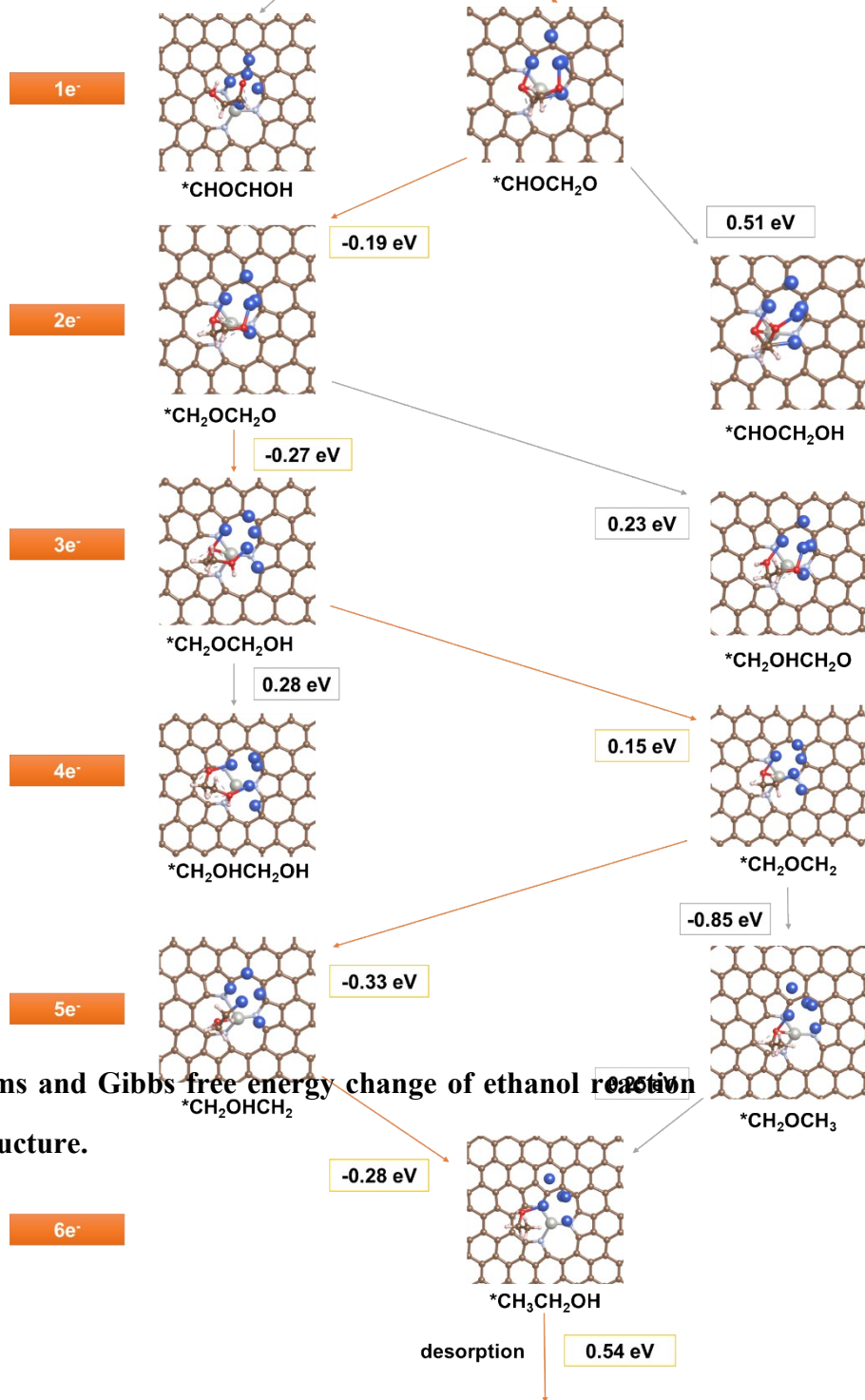


Fig. S22 Schematic diagrams and Gibbs free energy change of ethanol reduction pathway on Cu/PdN₃-pl structure.

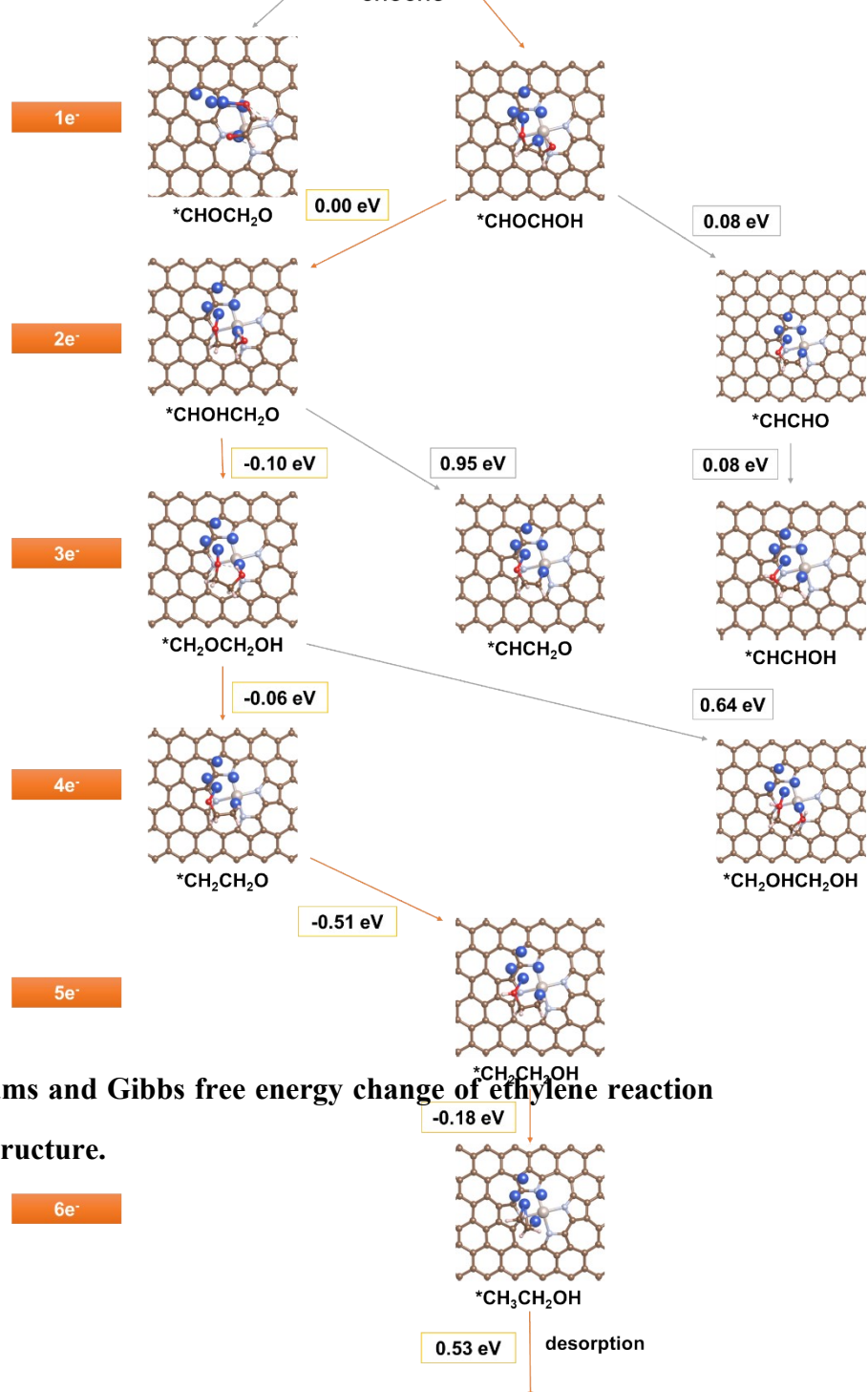


Fig. S23 Schematic diagrams and Gibbs free energy change of ethylene reaction pathway on Cu/RuN₄-pl structure.

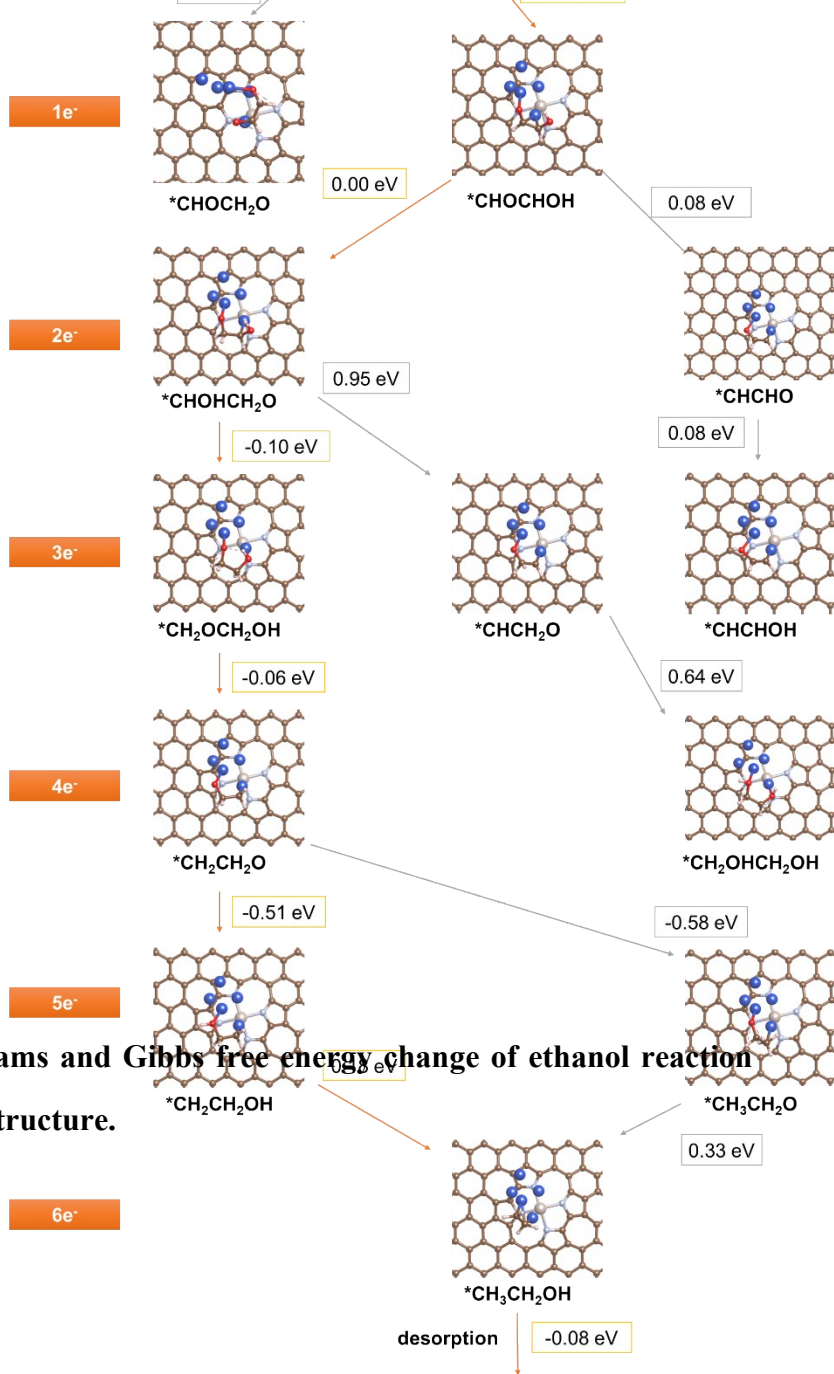
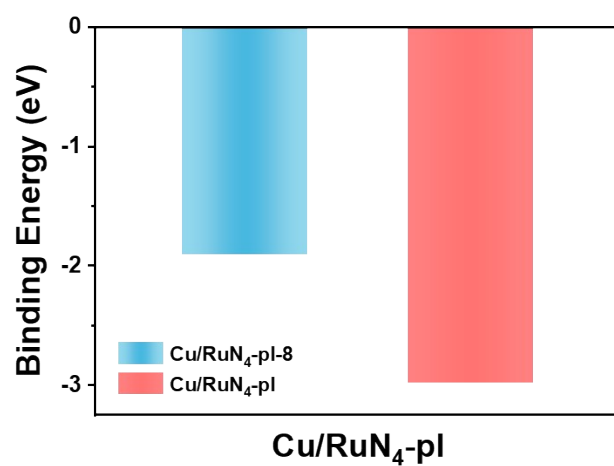


Fig. S24 Schematic diagrams and Gibbs free energy change of ethanol reaction pathway on Cu/RuN₄-pl structure.

(a)



(b)

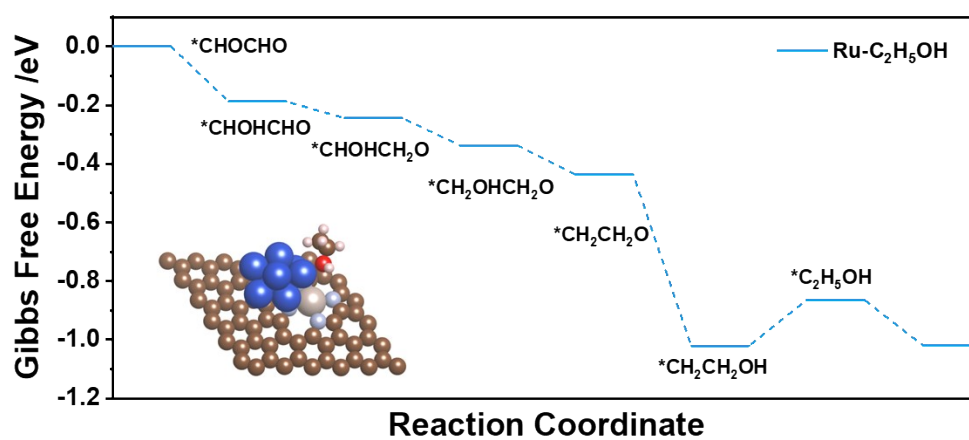


Fig. S25 (a) Comparison of binding energy between Cu/RuN₄-pl-8 and Cu/RuN₄-pl. (b) Gibbs reaction free energy diagrams for the ethanol pathway of Cu/RuN₄-pl-8.

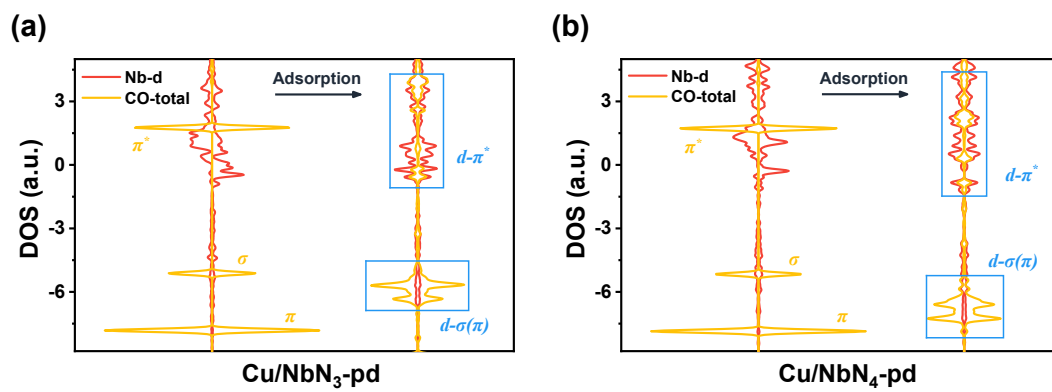


Fig. S26 DOS of before and after CO₂ adsorption on (a) Cu/NbN₃-pd and (b) Cu/NbN₄-pd.

Table S1. Bader charge data of Cu/NbN₃-pd.

Atom	X	Y	Z	CHARGE	Atom	X	Y	Z	CHARGE
C1	0.03	1.46	1.97	4.08	C41	6.20	7.83	2.23	4.11
C2	1.26	0.76	1.97	3.91	C42	7.48	7.14	2.04	3.44
C3	2.50	1.47	2.01	3.97	C43	8.68	7.88	1.88	4.13
C4	3.73	0.75	1.99	3.99	C44	9.91	7.17	1.83	3.88
C5	4.96	1.45	2.07	4.11	C45	-4.91	10.02	1.86	3.96
C6	6.19	0.74	2.04	3.88	C46	-3.68	9.30	1.82	4.16
C7	7.43	1.45	2.07	3.99	C47	-2.44	10.02	1.84	3.79
C8	8.66	0.75	1.99	3.94	C48	-1.21	9.30	1.83	3.95
C9	9.89	1.47	2.00	4.15	C49	0.03	10.02	1.87	4.14
C10	11.13	0.76	1.97	3.96	C50	1.26	9.30	1.88	3.96
C11	12.36	1.46	1.97	4.17	C51	2.49	10.02	1.92	3.96
C12	13.60	0.75	1.97	3.76	C52	3.72	9.31	1.97	4.13
C13	-1.21	3.60	1.91	3.95	C53	4.97	10.01	2.02	3.93
C14	0.03	2.89	1.96	4.16	C54	6.20	9.29	2.09	4.01
C15	1.27	3.60	1.99	3.93	C55	7.43	10.01	1.99	4.03
C16	2.52	2.90	2.07	3.99	C56	8.67	9.30	1.90	3.95
C17	3.76	3.62	2.20	4.11	C57	-6.15	12.15	1.94	3.74
C18	4.99	2.86	2.27	3.51	C58	-4.91	11.44	1.90	4.17
C19	7.40	2.87	2.24	3.56	C59	-3.68	12.15	1.92	3.97
C20	8.63	3.62	2.14	4.12	C60	-2.45	11.44	1.89	4.13
C21	9.87	2.90	2.02	3.92	C61	-1.21	12.15	1.94	4.08
C22	11.12	3.60	1.94	4.10	C62	0.03	11.44	1.91	3.94
C23	12.36	2.89	1.93	3.96	C63	1.26	12.15	1.94	3.74
C24	-2.44	5.74	1.84	3.72	C64	2.49	11.44	1.94	4.17
C25	-1.21	5.02	1.87	4.17	C65	3.73	12.15	1.96	3.96
C26	0.02	5.74	1.88	3.96	C66	4.96	11.44	1.98	4.16
C27	1.25	5.02	1.95	4.13	C67	6.19	12.15	1.98	3.90
C28	2.48	5.74	1.99	3.99	C68	7.43	11.44	1.96	4.08
C29	3.70	5.05	2.17	3.45	C69	5.02	4.09	5.06	3.52
C30	8.68	5.06	2.04	3.50	N1	6.19	3.47	2.53	6.20
C31	9.91	5.74	1.87	4.03	N2	4.83	5.80	2.37	6.28
C32	11.14	5.02	1.87	3.96	N3	7.54	5.79	2.18	6.24
C33	-3.67	7.88	1.80	4.07	Nb	6.21	5.21	3.79	11.33
C34	-2.44	7.16	1.81	3.91	Cu1	5.16	6.00	5.89	10.96
C35	-1.21	7.88	1.82	4.16	Cu2	4.12	8.14	5.55	11.02
C36	0.02	7.16	1.85	3.96	Cu3	6.21	8.00	4.39	10.85
C37	1.25	7.88	1.89	4.17	Cu4	7.65	6.48	5.60	11.20
C38	2.48	7.17	1.96	3.73	Cu5	6.14	7.97	6.81	11.02
C39	3.71	7.88	2.00	4.01	O	4.39	3.19	5.53	7.09
C40	4.91	7.15	2.16	3.60					

Table S2. Bader charge data of Cu/NbN₄-pd.

Atom	X	Y	Z	CHARGE	Atom	X	Y	Z	CHARGE
C1	0.04	1.56	2.00	3.99	C40	7.35	7.19	1.99	4.12
C2	1.27	0.84	2.00	3.95	C41	8.60	7.91	1.97	3.84
C3	2.52	1.55	2.03	4.06	C42	9.85	7.22	1.97	3.89
C4	3.73	0.80	2.02	4.14	C43	-4.94	10.07	1.95	3.74
C5	4.97	1.51	2.02	3.98	C44	-3.71	9.36	1.94	4.16
C6	6.20	0.80	1.98	3.99	C45	-2.47	10.07	1.93	3.97
C7	7.43	1.51	1.98	3.95	C46	-1.23	9.37	1.90	4.17
C8	8.67	0.81	1.96	3.98	C47	0.00	10.09	1.90	3.79
C9	9.90	1.53	1.98	3.97	C48	1.23	9.39	1.89	3.99
C10	11.14	0.83	1.97	3.73	C49	2.47	10.10	1.94	4.19
C11	12.38	1.54	1.98	3.89	C50	3.71	9.41	1.95	4.01
C12	13.61	0.84	1.98	4.08	C51	4.94	10.10	1.92	3.98
C13	-1.19	3.68	1.97	3.93	C52	6.17	9.37	1.92	3.99
C14	0.07	2.99	2.00	3.96	C53	7.41	10.08	1.94	3.96
C15	1.32	3.71	2.03	3.95	C54	8.63	9.35	1.95	4.15
C16	2.57	2.98	2.10	3.62	C55	-6.15	12.23	1.97	3.96
C17	4.97	2.92	2.11	3.44	C56	-4.93	11.50	1.97	3.94
C18	6.21	3.63	2.10	3.69	C57	-3.69	12.21	1.98	3.94
C19	7.43	2.93	2.02	3.97	C58	-2.46	11.50	1.95	3.96
C20	8.66	3.65	2.02	3.86	C59	-1.22	12.21	1.95	4.18
C21	9.90	2.95	2.00	4.17	C60	0.01	11.51	1.93	3.91
C22	11.13	3.67	1.98	3.96	C61	1.25	12.22	1.94	4.25
C23	12.38	2.97	1.98	4.15	C62	2.48	11.52	1.94	3.93
C24	-2.46	5.81	1.93	4.31	C63	3.72	12.23	1.95	3.95
C25	-1.21	5.10	1.93	4.09	C64	4.96	11.52	1.94	4.18
C26	0.02	5.82	1.89	3.75	C65	6.20	12.24	1.95	3.86
C27	1.28	5.14	1.94	3.64	C66	7.42	11.51	1.96	4.15
C28	7.36	5.75	2.07	3.45	C67	4.98	4.54	4.65	3.43
C29	8.62	5.07	2.02	3.95	N1	3.79	3.63	2.23	6.21
C30	9.86	5.80	1.98	4.21	N2	2.45	5.88	1.94	6.34
C31	11.11	5.09	1.96	3.88	N3	6.19	5.01	2.21	6.27
C32	-3.72	7.93	1.94	3.95	N4	4.92	7.27	1.84	6.21
C33	-2.47	7.23	1.92	3.73	Nb	4.26	5.63	2.95	11.09
C34	-1.24	7.95	1.89	3.94	Cu1	4.36	6.25	5.42	10.97
C35	0.00	7.25	1.86	4.08	Cu2	2.02	6.67	5.37	11.03
C36	1.22	7.97	1.85	4.03	Cu3	3.48	8.13	4.14	10.86
C37	2.44	7.25	1.88	3.59	Cu4	5.57	8.28	5.36	11.00
C38	3.71	7.97	1.96	3.74	Cu5	3.49	8.19	6.57	11.05
C39	6.13	7.94	1.91	3.58	O	5.49	3.63	5.23	7.05